Canadian Science Publishing | Canadian Geotechnical Journal

Demystifying basal pore pressure measurement in landslide flume experiments

Journal:	*Canadian Geotechnical Journal*
Manuscript ID	cgj-2024-0746.R1
Manuscript Type:	Research Article
Date Submitted by the Author:	22-Feb-2025
Complete List of Authors:	Fawley, Amanda; Queen's University, Department of Civil Engineering Taylor-Noonan, Alex; Queen's University, Department of Civil Engineering Tauskela, Lisa; Queen's University, Department of Civil Engineering Treflik-Body, Erica; Queen's University, Department of Civil Engineering Take, W. Andy; Queen's University, Department of Civil Engineering
Is the manuscript for consideration in a Special Issue or Collection?:	Not applicable (regular submission)
Keyword:	Landslide, flume, pore water pressure, landslide mobility

Demystifying basal pore pressure measurement in landslide flume experiments

A. Fawley[1], A. Taylor-Noonan[2], L. Tauskela[3], E. Treflik-Body[4], and W. A. Take[5]

[1] Research Student, GeoEngineering Centre at Queen's-RMC, Department of Civil Engineering, Queen's University, Kingston, Ontario, Canada. (ORCID: 0009-0000-6509-2573) (16adrf@queensu.ca)

[2] Researcher, GeoEngineering Centre at Queen's-RMC, Department of Civil Engineering, Queen's University, Kingston, Ontario, Canada. (ORCID: 0000-0002-5590-7350) (18amtn@queensu.ca)

[3] Research Student, GeoEngineering Centre at Queen's-RMC, Department of Civil Engineering, Queen's University, Kingston, Ontario, Canada. (lisa.tauskela@queensu.ca)

[4] Research Student, GeoEngineering Centre at Queen's-RMC, Department of Civil Engineering, Queen's University, Kingston, Ontario, Canada. (ORCID: 0000-0003-3013-3448) (erica.treflikbody@queensu.ca)

[5] Professor & Canada Research Chair in Geotechnical Engineering, GeoEngineering Centre at Queen's-RMC, Department of Civil Engineering, Queen's University, Kingston, Ontario, Canada (ORCID: 0000-0002-8634-1919) (andy.take@queensu.ca)

Corresponding author: W. Andy Take (andy.take@queensu.ca)

Keywords

Landslide, flume, pore water pressure, landslide mobility

Abstract

Laboratory landslide flume have revealed that saturated granular flows experience greater mobility than their dry counterparts, being notably faster, farther reaching, and experiencing enhanced spreading. The ability to reliably measure basal pore water pressures is critical for developing, evaluating, and validating constitutive relationships linking the effects of pore pressure to the mechanisms causing increased mobility. Unfortunately, experience has shown that two identical sensors installed in the base of a landslide flume can yield wildly different responses to the same multi-phase landslide. In this paper we explore the hypothesis that the elevation of pore water pressure sensor filter elements can influence sensor readings. A unique experimental strategy of simplifying the flow into a single fluid phase is used to validate sensor readings, prior to application in multi-phase flows. Dam-break releases of 600 kg of water at the top of the inclined flume slope are used as a parametric study to provide evidence to support the hypothesis that sensor roughness significantly impacts the pore pressure recorded in high velocity flows. These results are then contrasted to observations of releases of multi-phase flows to derive best practices for the reliable measurement of pore pressure in landslide flume tests.

1. Introduction

Landslides are dangerous, global phenomena that can occur in a range of environments and commonly result in loss of life, destruction of resources, and high financial loss. They can be characterized as a partially to fully saturated mass of material (earth, rock, or debris) moving rapidly to slowly downhill under the influence of gravity (Cruden 1991; IPCC et al. 2012). Managing landslide risk requires the ability to predict the size and location of a landslide, and the resulting mobility (velocity, flow depth, and runout) that define the extent of the hazard (e.g. Dai et al. 2002; Cuomo et al. 2014; Choi and Nikooei 2023). The dangerous and unpredictable nature of these events make them difficult to quantitatively observe during triggering and subsequent flow in the field. Instead, laboratory flume tests have enabled researchers to safely study landslides in an environment that allows key variables to be independently controlled and for the complex behaviour of granular flows to be simultaneously captured using multiple types of instrumentation. This allows the research community to compare and contrast highly detailed observations of physical laboratory flows to the results of proposed numerical simulation methods and further the development of numerical, constitutive and rheological, and mathematical prediction models. A key parameter defining the mobility of a landslide is the spatially and temporarily varying pore pressure within the debris. Despite the significance of this variable, laboratory landslide flume experiments on dry materials still tend to largely outnumber experiments on saturated flows in the literature. The dearth of published data on pore pressures at the base of saturated flows is at least partially due to the extreme difficulty in measuring this parameter in fast-moving multiphase flows.

Basal pore pressure transducers (PPT) are sensors installed into the flume base to record the pore water pressure along the slip surface within the laboratory landslide experiment. Given that the role of a PPT is to measure only the fluid pressure component of stress, a filter element is typically installed between the flow and the pressure sensing diaphragm of the sensor. Researchers have utilized a variety of filter types in landslide tests including, but not limited to, saturated ceramic filters (e.g. Ooi et al. 2014; Ng et al. 2016), filter paper (e.g. Montrasio and Valentino 2007), membranes with underlying fluid reservoir to interact with

the sensor diaphragm (e.g. Kaitna et al. 2016), and 3D printed resin caps with symmetrical holes (e.g. Tauskela 2022; Taylor-Noonan et al., 2022).

Anecdotal experience suggests that two neighbouring and seemingly identical PPTs in a flume can have markedly different responses as illustrated schematically in Figure 1. One sensor may record pore water pressure greater than hydrostatic (Figure 1a), whereas its neighbour may register suction (Figure 1b). The correct reading in this case is ambiguous and neither reading may be accurate. Confusing results, like those in Figure 1, are often omitted in publications since there is understandable skepticism regarding the validity of the measurements.

After a decade of experimentation and trial and error in pore pressure measurement, we hypothesize that the explanation for the behaviour illustrated schematically in Figure 1, is the result of pressure fields created by flow separation if the PPT filter cap is not perfectly flush with the flume base. Support to explore this hypothesis can be found in the fluid mechanics literature regarding high velocity flows over cylindrical protrusions and cavities. For the case of an elevated protrusion, flow separation has been observed to be dependent on the submergence of the protrusion, the protrusion size, the Reynolds number (Re), and flow state (i.e. steady vs unsteady) (e.g. Hain et al. 2008; Sadeque et al. 2008; Rostamy et al. 2012; Fanini Leite and Avelar 2016). The flow separation creates flow structures and fields, varying vortices, and wakes in front, around, behind, and on top of the cylinder. These turbulent regions exert varying magnitudes of pressure on the protrusion with the possibility of developing pressures below atmospheric (Sadeque et al. 2008). For the case of flow over a circular cavity, the pressure in the cavity has been shown to be a function of the aspect ratio (AR) between the height and diameter of the cavity, the Re, and flow state (Pozrikidis 1994). Inspired by these studies, Figure 2 illustrates conceptually how a recessed (Figure 2a) or protruding (Figure 2b) filter cap may cause flow separation and unexpected pressure readings measured by PPT sensor. The resulting turbulence may cause a higher than expected pressure for the case of a recessed filter, or a lower than expected pressure for the case of a protruding filter.

The objectives of this paper are 1) to test the hypothesis by performing an experimental parametric study on PPT sensors installed at a range of different positions from raised, to flush, to recessed; and 2) to develop

best practices that can be used by the landslide research community to validate pore pressure sensor installations in landslide flume experiments to increase confidence in measurements. To accomplish these objectives we adopt a two-stage experimental strategy of first simplifying the flow into a single fluid phase to test the hypothesis against independent flow height observations before exploring the phenomena in multi-phase flows.

2. Materials and Methods

2.1. Landslide Flume

Tests were conducted in the Queen's University landslide flume. Given that the majority of landslide experiments used to model runout distance are unsteady channel flume experiments, we have selected this style of apparatus in which to explore pore pressure measurement effects. As displayed in Figure 3, the flume is 2.09 m wide with an 8.23 m long aluminium slope inclined at 30° from horizontal and features a 33 m long horizontal runout zone. The 8.23 m slope and the first 3.68 m of the runout zone is aluminum with glass side walls to allow the flow to be observed. The remaining runout zone is smooth concrete with brick sidewall and occasional windows for viewing flow. The release box located at the top of the slope can accommodate over 1.0 m^3 of water or saturated material. All tests were initiated by opening its hinged door rapidly with pneumatic cylinders.

2.2. Instrumentation

2.2.1. Pore Water Pressure

In this study, the two PPTs (model LM37-00000F-002PG, TE Connectivity) used to measure the basal pore water pressure were installed to be integral with the base of the flume, with a rigid connection that remained serviceable for cleaning. The base of the flume consists of 25 mm aluminum plate with 1/4"-19 British Standard Pipe Parallel (BSPP) threaded holes along the slope centerline at 2.89 m (PPT 1) and 1.69 m (PPT 2) from the slope base respectively. Given that the release height is in the flume is fixed, choosing two measurement locations at different travel distances down the flume permits a preliminary exploration of the

effect of flow velocity. With a pressure head range of 0 to 13.9 kPa, the sensors, supplied with 5 Volts (V), record the pressure exerted on their diaphragms and output a corresponding reading from 0.5 - 4.5 V to an accuracy of ±1% of full-scale. These voltage readings are recorded by a data acquisition system at a frequency of 500 Hz. These readings can then be converted, using a linear calibration, into water head (cm). The chosen sensors featured larger threads (1/2"-14 NPT) than the holes drilled in the aluminum flume base (1/4"-19 BSPP). 1/4"-19 BSPP to 1/2"-14 NPT steel adaptors were used to install the PPTs in the flume which facilitated sensor removal, cleaning, saturation, and consistent installation between tests.

The filters used for testing were 3D printed resin caps 13.1 mm in diameter, 10 mm tall, and with seven 1.5 mm diameter holes evenly spaced along its top. They regulated fluid infiltration and prevented granular material from making contact with the PPT diaphragm during testing. Critically, these caps were designed with the BSPP parallel threads to enable precise control of the elevation of the cap following installation. These caps were installed above the PPTs and sanded down so they were flush with the slope surface. Increments of cap rotation were then used to impose precise changes in cap elevation. The complete PPT, adaptor, and filter setup is displayed in Figure 4.

2.2.2. Flow Height

To place the pore water pressure measurements in context, the flow height was measured in two different ways – ultrasonic distance sensors along the flume centreline and through images captured at the side wall of the flume by high speed cameras. The ultrasonic distance sensors (model S18UUAQ, Banner Engineering Corp., 2.5 ms response time) were positioned 28 cm above each PPT and recorded the bed-normal flow height via pulses of ultrasonic energy reflected off either water or granular material. In the water flows, this recorded flow height (Z) is equal to the water height (Z_W). Within the saturated granular flows, the water height (Z_W) was not constantly equal to the total flow height (Z), hence the ultrasonics were only used to capture the total flow height (Z) and we utilized high speed cameras to capture the side profile of the flow and observe the relative height of water (Z_W) in the total flow height (Z) in line with both PPTs. Images were captured at 50 frames per second (fps) for water tests (Figure 5b) and 115 fps for the

saturated granular tests (Figure 5c). The camera system was synchronized with the main data acquisition system such that comparisons can be made to the PPT and ultrasonic sensor data.

2.2.3.Flow Velocity

The high speed images were also used to obtain the surface velocity at each PPT in the saturated granular tests using particle image velocimetry (PIV). PIV is a velocity-measuring procedure that gathers displacement data from a series of images. It processes the images by dividing each into a series of patches with specific coordinates, called the static mesh. These patches are then compared to the patches in the subsequent image and the difference in location coordinates is recorded. This continues for all provided images and then a displacement profile is generated displaying the displacement for each patch (White et al. 2003). This displacement can then be used to create a velocity profile of the flow. Using this procedure yielded a mean flow velocity about 4 m/s and 5 m/s passing over PPT 1 and PPT 2 respectively for the saturated granular tests.

The flow velocity in the water tests was obtained by observing the flow displacement in relation to references in the recorded data. From this, the mean flow velocities were about 6.1 m/s and 7 m/s, passing over PPT 1 and PPT 2 respectively.

2.2.4.Flow conditions

The flow conditions in these experiment sets can be described with the Reynolds (**Re**) and Froude (**Fr**) numbers, which define the turbulence and state of the flow (subcritical or supercritical) based on the ratios of inertial forces to viscous forces and gravity forces, respectively (e.g. Faug 2015).

[1] $$\boldsymbol{Re} = \frac{\boldsymbol{\rho V R}}{\boldsymbol{\mu}}$$

[2] $$\boldsymbol{Fr} = \frac{\boldsymbol{V}}{\sqrt{\boldsymbol{gZcos\theta}}}$$

Where ρ is the density of the fluid (kg/m^2), V is the mean flow velocity (m/s), μ is the dynamic viscosity of the fluid (Pa·s), g is the gravitational acceleration of earth (m/s^2), Z is the hydraulic depth (m), and θ is the flume slope. R is the hydraulic radius of the rectangular flume channel of width b:

[3] $$\boldsymbol{R = \frac{bZ}{(b+2Z)}}$$

Smaller flumes are typically associated with lower **Re** values as both flow velocity and depth are typically lower. Landslide experiments would intend for supercritical flows, that is, **Fr** > 1.

2.3. Materials

The single fluid phase test series used 0.6 m^3 water flows to avoid the complexity of granular-fluid interactions. The multi-phase test flows were comprised of water and pseudo-spherical (92% sphericity) ceramic granules 3.85 ± 0.41 mm in grain diameter, a grain density of 2241 kg/m^3, and hardness greater than 6.5 on Mohr's scale (Coombs et al. 2020). These granules were selected based on prior test evidence that they generate minimal excess basal pore water pressure during fast flows (Kimball 2021; Taylor-Noonan et al. 2022). Water was added to fill the pore spaces after the granules were levelled resulting in a total saturated granular flow volume of 0.6 m^3 with 840 kg of ceramic granules and 231 L of water.

The water added to the release box was measured using a flow meter (FLOMEC© TM Series© totalizer) with a reading accuracy of ±3%. The water was sourced from the municipal supply.

2.4. Test Procedure

Prior to each test, the sensor caps were adjusted to the desired elevation and then saturated with water to mitigate any trapped air in the void space between the filter and PPT diaphragm or possible lag upon arrival of the flow. The baseline reading was set with the water level at the flume surface.

A total of 94 experiments were conducted to explore recessed and raised sensor cap elevations (H) for ranging from -5.0 mm to 2.66 mm, with a minimum of two water tests conducted at each elevation. One saturated granular test was run for H at -1 mm and 1 mm, and two tests at 0 mm. A complete summary of experiments is outlined in Table 1. There are some instances where material volume varies, however these results were not included in the final analysis since the focus was on a constant flow volume.

3. Effects of Sensor Cap Elevation on Basal Water Pressure in Water Flows

The first set of experiments used 0.6 m^3 of water for each flow to explore the hypothesis using flows where the expected pressure is known. From Chow (1959), the fluid pressure head (h) at the base of steady water flows traveling down a slope (θ) can be related to the gravity-normal flow height y or the bed-normal flow height (Z) as illustrated on Figure 5a:

[4] $$\boldsymbol{h = y\cos^2\theta = Z\cos\theta}$$

Throughout the remainder of this paper, the recorded pressure head (h) is converted to bed-normal water head (Z_{PPT}) for the purposes of comparison with the bed-normal water height (Z_W) recorded by the ultrasonic sensors in the water flows and identified via high speed imagery in the saturated granular flows.

3.1. Basal Pore Water Pressure and Ultrasonic Sensor Data Observations

The effects of sensor cap elevation (H) are reviewed as flush, recessed, and raised scenarios. In the flush scenario (Figure 6a and repeated as Figure 7a), the PPT 1 water head measurements are close to those expected from the Ultrasonic Sensor 1 flow depth measurements (via Eq. 1). There appears no delay between flow arrival (via flow depth) and rise in pressure head. This is confirmation that the installing sensor caps flush with the flume surface is appropriate for measuring the basal pore pressure of these dynamic releases.

Figure 6 compares the results as the sensor cap is successively moved downwards (further recessed) over the range of 0 mm (flush) to -5.0 mm. At slight recessions, the PPT was observed to record a water head greater than the ultrasonic sensor (Figure 6b), even measuring over seven times greater than the actual flow height at the -0.67 mm configuration (Figure 6c).

The pressure head at the PPT decreased as the cap was recessed further. When set at H = -2.33 mm (Figure 6d), the system again measured pressure head results similar to the actual flow depth. We term this a 'false positive'. Further movements (Figure 6e) resulted in further decreased measurements but the measured response remained above atmospheric.

In contrast, the PPTs with a raised cap registered progressively greater negative responses with each increment added to the cap elevation (Figure 7). For H > 2 mm, the pressure at the PPT became so low that the sensor was under range during portions of the flow and did not return a voltage. This precluded tests with a further increase in H.

3.2. Sensor Amplification Ratio

The Sensor Amplification Ratio (r_h) is a unitless value created to compare the PPT data to the actual water depth. Following Eq. 2, we define r_h to be the ratio of mean bed-normal head measurements from the PPT ($\overline{Z}_{PPT}$) and mean water depth measurements ($\overline{Z}_W$) for a specified time frame:

$$[5] \qquad \boldsymbol{r_h = \frac{\overline{Z}_{PPT}}{\overline{Z}_W}}$$

The process involved identifying a time frame for each test at a H where a sustained maximum was observed (t_1 to t_n on Figure 8). The ratio was calculated at each 0.002 s time step and the mean of all these ratios were taken as the final representative value, r_h. Time intervals of sensor dropouts were omitted during this process.

At $r_h = 1$, the PPT sensors are reading 'true' to expectations. For $r_h > 1$, the PPT sensors are over-reporting fluid pressure. For $0 < r_h < 1$, the PPT sensors are under-reporting fluid pressure. For $r_h < 0$, the sensors are reporting pressures below atmospheric (suction).

r_h for each water test was plotted against the respective sensor cap elevations and a non-linear trendline for the data was produced (Figure 9). Ratios for both PPTs displayed similar responses to the raised and recessed conditions, however PPT 2 (Figure 9b) was observed to have larger r_h's than PPT 1 (Figure 9a) and there were also some differences between trendlines. This implies that r_h may be influenced by the flow velocity, as the flow accelerated between PPT 1 and PPT 2, or that flow separation caused by PPT 1 is influencing readings downstream at PPT 2.

3.3. Behaviour without a sensor cap

As water tests do not require a filter for the purposes of screening out granular material, it was explored if a filter is still necessary for accurate measurements given that readings for deeply recessed caps were registering close to the Base case. Two tests were conducted without the resin filter, which resulted in the 1/4”-19 BSPP threaded hole exposed above the PPTs. The results, also on Figure 9, show r_h exceeding 2.

For water flows, the mean flow velocity was between 6 m/s and 7 m/s based on the difference in time-of-arrival at the ultrasonic sensors. For the water flows **Re** of 2.7×10^5 and 2.6×10^5 and **Fr** of 8.51 and 10.75 were found at PPT 1 and PPT 2, respectively. Variables used in these calculations are outlines in Table 2. These values indicate that flow passing over each sensor was turbulent and supercritical.

4. Effects of Sensor Cap Elevation on Basal Water Pressure in Saturated Granular Flows

The velocity and pressure regime in a wet granular flow can be influenced by the contraction or dilation of the granular particles, and fluid drag where the relative speeds of the phases differ. The next series of tests was conducted to evaluate if the observed sensor behaviour of the water tests, namely over-reporting pressure, under-reporting pressure, and reporting negative pressure, would occur in a wet granular flow and if so, to what extent. Fully saturated granular tests were run with the caps set at H = ±1 mm and flush configurations. This flow was expected to have a lower velocity and experience segregation between the particles and water due to their contrasting material properties.

The top of fluid and top of particles was not concurrent in the wet granular flows (Figure 5c); therefore, PPT measurements were compared to the actual water height (Z_W) identified in the high speed camera flow profile. Further, the ultrasonic sensors, which could only measure top of the flow, were in reasonable agreement with the flow height measurements obtained using the high speed cameras.

The recessed test, in Figure 10b, displayed the same phenomenon as its water counterpart displayed in Figure 10a. While the magnitude was diminished in comparison, the PPT recorded greater water head than the actual water height. The raised granular test, in Figure 11b, experienced the same suction that its water counterpart did in Figure 11a. The flush test in Figure 12b indicated that the upper bounds of the PPT

measurements corresponded to the actual water height (Z_W), and it confirmed this configuration works for both the granular and water (Figure 12a) tests.

These saturated granular flows, the mean flow velocity was estimated as 4 m/s and 5 m/s for PPT 1 and PPT 2 respectively using high speed images and making reference to the velocity profile for a 0.6 m^3 flow of the same materials in the same flume from Taylor-Noonan et al. (2022). From this, **Re** = 3.4×10^5 at both PPT locations. **Fr** = 5.37 and 7.44 at PPT 1 and PPT 2, respectively. Table 2 provides a summary of these results and the associated variables used in their calculations.

5. Discussion

The only tests where the PPT and ultrasonic sensor data consistently matched was when the cap was completely flush with the flume surface following meticulous sanding. This was defined as the Base case and is considered the ideal cap setup for testing in the given laboratory flume conditions. For raised caps, the water flows exhibited decreasing measured water head with increasing cap protrusion height. This observation is in line with the expected hypothesis of flow separation and a turbulent low pressure zone forming above the sensor cap (Figure 2b). We also qualitatively observed this behaviour in earlier tests when an obstruction or irregularity is present immediately upstream of the PPT. To ensure the cap is flush with the flume in the Base case, sandpaper was used to smooth the cap surface and remove irregularities on the flume surface around and ahead of the cap.

From the water tests with an increasingly recessed cap, the observed behaviour is highly non-linear and suggests a transition with cavity geometry (Figure 9). The slightest cap recession distances (less than a millimetre) resulted in the highest pore pressure measurements. This is attributed to impact forces with the exposed sidewall of the cavity. Beyond a recession distance of 0.7 mm, the pressure decreases until asymptotically approaching $r_h = 0.6$. The observations are in line with the development of a recirculation vortex within a cavity of sufficient height relative to its diameter (the aspect ratio AR) which decreases the magnitude of stress on the bottom of the cavity. Beves et al. (2004) found flow separation within the cavity at an AR > 0.22, but also that the radius of the edges of said cavity can influence the flow separation point.

Ravulapati (2014) found this flow separation can result in the formation of a flow structure and vortices, however a predominant flow structure is not always distinguishable for shallow cavities. Here, we noted the behaviour at 0.5 mm recession distance of the 13.1 mm diameter cap (AR = 0.04).

The pressure measurements observed may be the summation of both the impact forces and a developing recirculating flow structure. The 'false positive' observed for the -2.33 mm recessed test was likely the coincidental negative superposition of these behaviours. It is not recommended for an experimental setup to rely on this 'false positive' as it is likely dependent on both the experimental setup and flow velocity.

Strictly speaking, the fluid ports on the sensor caps would also act as recessed cavities. In this study, the ports were kept small leading to high AR. The absolute diameter of the hole may limit the formation of the recirculation vortex. Shaw (1960) found that smaller hole diameters were most accurate for static pressure measurements. For dynamic pressure measurements such as landslides, small diameter fluid ports should be checked that they do not attenuate the rising pressure upon landslide arrival. This involves investigating whether the hydraulic conductivity of water passing through the filter is slowed to the extent that the measurement is delayed or dampened due to pressure dissipation before reaching the sensor.

Conversely, the 'no cap' test was another example of a large diameter, high-AR cavity. The sensors read r_h exceeding 2, surprisingly high for a high-AR cavity. The flow pattern for this complicated cavity geometry may be beyond the original hypothesis of this study. These results do however confirm that the interface with the flow should be smooth as possible and kept reasonably small.

In the saturated granular tests, the same phenomena were observed for the tests on each cap elevation despite the presence of granular material and slower mean flow velocity. We postulate that the slower flow velocity contributed to the diminished absolute magnitude of r_h. The granules themselves may also interrupt formation of the flow structures discussed above for water flows. The higher frequency fluctuations displayed by the PPT data in the granular flows were likely caused by the collisions of the granules in the flow and may have been exacerbated by vibrations of the flume itself (Taylor-Noonan et al., 2022). The PPT results from the flush configuration tests demonstrate this method is applicable to granular flows but data filtering methods will be required to remove the noise and observe the representative pore pressure on

the basal plane. The vibration of the flume should be minimized and no data filtering used if the dynamic fluctuations are to be assessed.

The magnitude of r_h expected from sensor cap miscalibration is likely specific to not only the experimental setup but the nature of the flow released. Additional research is needed with varying flow velocities to permit a broader discussion of how the behaviour identified scales from small laboratory flumes to full-scale flows. In the present study, both the water and saturated granular flows were found to be supercritical and turbulent at both sensor locations with their **Re**'s ranging from 2.6×10^5 to 3.4×10^5 and **Fr**'s from 5.37 to 10.75. The laboratory flume used was able to produce a flow with similar **Re** to the USGS Flume Debris Flows ($\mathbf{Re} = 3 \times 10^5$), but two to five orders of magnitude less than the three field flows as tabulated by Iverson and Denlinger (2001). The **Fr** was similar to the USGS experimental flows ($\mathbf{Fr} = 10$) and two field debris flows ($\mathbf{Fr} = [3, 6]$) tabulated by Turnbull et al. (2015). Further work, using a different apparatus capable of source volumes with differing potential energy (i.e., release points) is therefore required to vary flow velocity to permit an exploration of how pore pressure measurements are influenced by **Fr** and **Re**.

In the present study, the base of the flume was a 25 mm thick aluminum plate, representing a smooth basal surface. This inevitably leads to inquiry regarding what may happen along a rough boundary. In particular, the observation that a protrusion or recess of a fraction of a millimetre can cause localized pore pressure effects suggests there needs to be further consideration regarding measuring pore pressures in laboratory settings. Firstly, these observations indicate that the localized pore pressure in front or behind an element of surface roughness (e.g., high point or low point) will be influenced by turbulence. This raises difficult questions regarding where the most appropriate location of a point measurement of pore pressure should be in such a situation. Secondly, and more fundamentally, these observations lead to questions regarding the definition of pore pressure for use in fast moving granular flows. Similar to the use of the concept of effective stress being defined as a smoothed approximation of normal contact forces across a plane, the representative pore pressure acting on a basal plane of a fast moving flow may also need spatial smoothing. In other words, a single point measurement of pore pressure, similar to a single point measurement of contact force, may not be fully representative of the "effective or average" pore pressure acting on the plane.

Further work is recommended to expand the work begun in the present study to explore surface roughness effects with different sized filter elements to spatially average pore pressure readings.

6. Conclusion

Fast-moving landslides are the product of multiple processes of interaction between particles and fluid. Both field observations (instrumented channels) and laboratory landslide flume tests are essential for observing the summation of these physical processes as the resulting pore water pressure. Such measurements are vital to develop understanding of the role of pore water pressure plays in landslide mobility and verify existing and novel analysis tools to predict, assess, and mitigate fast-moving flows in the field.

We hypothesised that error in PPT readings could be caused by flow separation around sensor components not installed completely flush with the flume. We systematically evaluated this by initially releasing many water flows. 94 tests releasing 0.6 m^3 of water were performed with a filter distance range of -5 mm to +2.64 mm. From this, we compared the PPT water head readings to the flow height. For recessed filters, the smallest recessed distances (-0.16 mm to -0.83 mm) resulted in the greatest water head readings, yielding results that were up to eight times greater than the measured hydrostatic. Further recession caused pressure readings to decrease. This behaviour is considered possibly due to the flow impact exerting large pressures on the base of the cavity (small magnitudes of recession) and due to a recirculation vortex forming within the cavity (larger magnitudes of recession). Conversely, raised filters displayed increasingly negative pressure readings in a non-linear trend, which is likely due to flow separation from the base of the flume. We observed that there is a highly non-linear error trend, and that the smallest recession or protrusion distances could result in some of the largest error (Figure 9). The same phenomena were clearly observed in the saturated granular tests, albeit to a lower magnitude.

For the first time, these observations provide an explanation regarding the challenges of measuring basal pore water pressure in high velocity, saturated landslide flume tests. While the magnitude of r_h is expected to be specific to the sensor setup and flow characteristics, the Base case of flush sensor filter caps is expected

to provide the most accurate measurements. Following the results of this study, we put forth some best practices for measurements.

Sensors should not be placed downstream of raised or recessed plates, bolts, edges of panels, other sensors, or any source of potential turbulence that could influence flow over the PPT. The results show that PPT 2, located downstream of PPT 1, could measure accurately when both sensors had flush caps. Sensor filter caps should be placed as flush as possible with the flume surface, with good results observed here after filling any low spots and sanding down any high spots. The cap design should be filter-compatible with the test media and promote the retention of water in the inclined orientation, prior to the start of the test.

The two series of tests showed that releasing water flows and comparing PPT readings to flow depth measurements provides a practical method for checking that basal pore water pressure sensor setup is suitable and readings are accurate. Water flows are more easily repeated, and the results here show that discrepancies are of a greater magnitude in water flows than saturated granular flows. Upon completion of successful water flows for validation, more confidence can be placed in basal PPT measurements in landslide studies.

Acknowledgements

This research was financially supported by the Natural Science and Engineering Research Council of Canada (NSERC) through Discovery Grant funding awarded to Take (RGPIN-2020-04077). Funding for the first author was provided in part through the Ontario Graduate Scholarship and the NSERC Canada Graduate Scholarship programs. The authors gratefully acknowledge the assistance of Josh Coghlan, Richard Foley, Artur Sass Braga and Meg McKellar in conducting the experiments in the laboratory.

Statements and Declarations

The authors declare there are no competing interests.

Data Availability Statement

Data generated or analyzed during this study is freely available in the Borealis Data Repository (https://doi.org/10.5683/SP3/OSHBNH) including videos capturing typical water flow and saturated granular flow experiments.

References

Armanini, A. 2013. "Granular flows driven by gravity." *J. Hydraul. Res.*, 51 (2): 111–120. Taylor & Francis. https://doi.org/10.1080/00221686.2013.788080.

Beves, C., Barber, T., and Leonardi, E. 2004. "An Investigation of Flow over a Two-Dimensional Circular Cavity." Sydney, Australia.

Choi, C. E., and Nikooei, M. 2023. "Revealing the physics of sediment ploughing by geophysical mass flows: Depth-averaged approach." Comput. Geotech., 154: 105119. https://doi.org/10.1016/j.compgeo.2022.105119.

Chow, V. T. 1959. "Basic Principals." Open-Channel Hydraul. New York: Blackburn Press.

Coombs, S. P., Apostolov, A., Take, W. A., and Benoît, J. 2020. "Mobility of dry granular flows of varying collisional activity quantified by smart rock sensors." *Can. Geotech. J.*, 57 (10): 1484–1496. NRC Research Press. https://doi.org/10.1139/cgj-2018-0278.

Cruden, D. M. 1991. "A simple definition of a landslide." *Bull. Int. Assoc. Eng. Geol. - Bull. Assoc. Int. Géologie Ing.*, 43 (1): 27–29. https://doi.org/10.1007/BF02590167.

Cuomo, S., Pastor, M., Cascini, L., and Castorino, G. C. 2014. "Interplay of rheology and entrainment in debris avalanches: a numerical study." Can. Geotech. J., 51 (11): 1318–1330. NRC Research Press. https://doi.org/10.1139/cgj-2013-0387.

Dai, F. C., Lee, C. F., and Ngai. Y. Y. 2002. "Landslide risk assessment and management: an overview." *Eng. Geol.*, 64 (1): 65–87. https://doi.org/10.1016/S0013-7952(01)00093-X.

Fanini Leite, H., and Avelar, A. 2016. "Investigation of Flow Patterns in Finite Cylinders." Vitória, ES, Brazil: 10.26678/ABCM.ENCIT2016.CIT2016-0667.

Faug, T. 2015. "Depth-averaged analytic solutions for free-surface granular flows impacting rigid walls down inclines." *Phys. Rev. E*, 92 (6): 062310. https://doi.org/10.1103/PhysRevE.92.062310.

Hain, R., Kähler, C. J., and Michaelis, D. 2008. "Tomographic and time resolved PIV measurements on a finite cylinder mounted on a flat plate." *Exp. Fluids*, 45 (4): 715–724. https://doi.org/10.1007/s00348-008-0553-x.

IPCC 2012. *Glossary of Terms*. A Special Report of Working Groups I and II of the Intergovernmental Panel on Climate Change [Field, C.B., V. Barros, T.F. Stocker, D. Qin, D.J. Dokken, K.L. Ebi, M.D. Mastrandrea, K.J. Mach, G.-K. Plattner, S.K. Allen, M. Tignor, and P.M. Midgley (eds.)], 555–564. Cambridge, UK, and New York, NY, USA: Cambridge University Press.

Iverson, R. M. 1997. “The Physics of Debris Flows.” *Rev. Geophys.*, 35 (3): 245–296. https://doi.org/10.1029/97RG00426.

Iverson, R. M., and Denlinger, R. P. "Flow of variably fluidized granular masses across three-dimensional terrain: 1. Coulomb mixture theory", *Journal of Geophysical Research: Solid Earth* 106, B1 (2001), pp. 537--552.

Kaitna, R., Palucis, M. C., Yohannes, B., Hill, K. M., and Dietrich, W. E. 2016. “Effects of coarse grain size distribution and fine particle content on pore fluid pressure and shear behavior in experimental debris flows.” *J. Geophys. Res. Earth Surf.*, 121 (2): 415–441. https://doi.org/10.1002/2015JF003725.

Kimball, J. 2021. “Large Scale Physical Modelling of Particle Size Segregation in Granular Flows.” Kingston, Ontario, Canada: Queen’s University.

Montrasio, L., and Valentino, R. 2007. “Experimental analysis and modelling of shallow landslides.” *Landslides*, 4 (3): 291–296. https://doi.org/10.1007/s10346-007-0082-3.

Ng, C. W. W., Kamchoom, V., and Leung, A. K. 2016. “Centrifuge modelling of the effects of root geometry on transpiration-induced suction and stability of vegetated slopes.” *Landslides*, 13 (5): 925–938. https://doi.org/10.1007/s10346-015-0645-7.

Ooi, G. L., Wang, Y.-H., Tan, P. S., So, C., Leung, M., Li, X., and Lok, K. 2014. “An Instrumented Flume to Characterize the Initiation Features of Flow Landslides.” *Geotech. Test. J.*, 37: 20130158. https://doi.org/10.1520/GTJ20130158.

Pozrikidis, C. 1994. “Shear flow over a plane wall with an axisymmetric cavity or a circular orifice of finite thickness.” *Phys. Fluids*, 6 (1): 68–79. American Institute of Physics. https://doi.org/10.1063/1.868046.

Ravulapati, K. 2014. “Separation Bubbles and Vortex Formation in Cavity Flows.” PhD Dissertations and Master’s Theses. Daytona Beach: Embry-Riddle Aeronautical University.

Rostamy, N., Sumner, D., Bergstrom, D. J., and Bugg, J. D. 2012. “Local flow field of a surface-mounted finite circular cylinder.” *J. Fluids Struct.*, 34: 105–122. https://doi.org/10.1016/j.jfluidstructs.2012.04.014.

Sadeque, F., Rajaratnam, N., and Loewen, M. 2008. “Flow around Cylinders in Open Channels.” *J. Eng. Mech.-ASCE*, 134. https://doi.org/10.1061/(ASCE)0733-9399(2008)134:1(60).

Shaw, R. 1960. The influence of hole dimensions on static pressure measurements. *Journal of fluid mechanics*, *7*(4), 550-564.

Tauskela, L. 2022. “Pore Pressure Dissipation And Reconsolidation Observed In Large Scale Experiments Of Liquefied Debris Flows.” Kingston, Ontario, Canada: Queen’s University.

Taylor-Noonan, A. M., Bowman, E. T., McArdell, B. W., Kaitna, R., McElwaine, J. N., and Take, W. A. 2022. “Influence of Pore Fluid on Grain-Scale Interactions and Mobility of Granular Flows of Differing Volume.” *J. Geophys. Res. Earth Surf.*, 127 (12): e2022JF006622. https://doi.org/10.1029/2022JF006622.

Turnbull, B., Bowman, E. T., and McElwaine, J. N. "Debris flows: Experiments and modelling", *Comptes Rendus Physique* 16, 1 (2015), pp. 86-96.

White, D. J., Take, W. A., and Bolton, M. D. 2003. “Soil deformation measurement using particle image velocimetry (PIV) and photogrammetry.” *Géotechnique*, 53 (7): 619–631. ICE Publishing. https://doi.

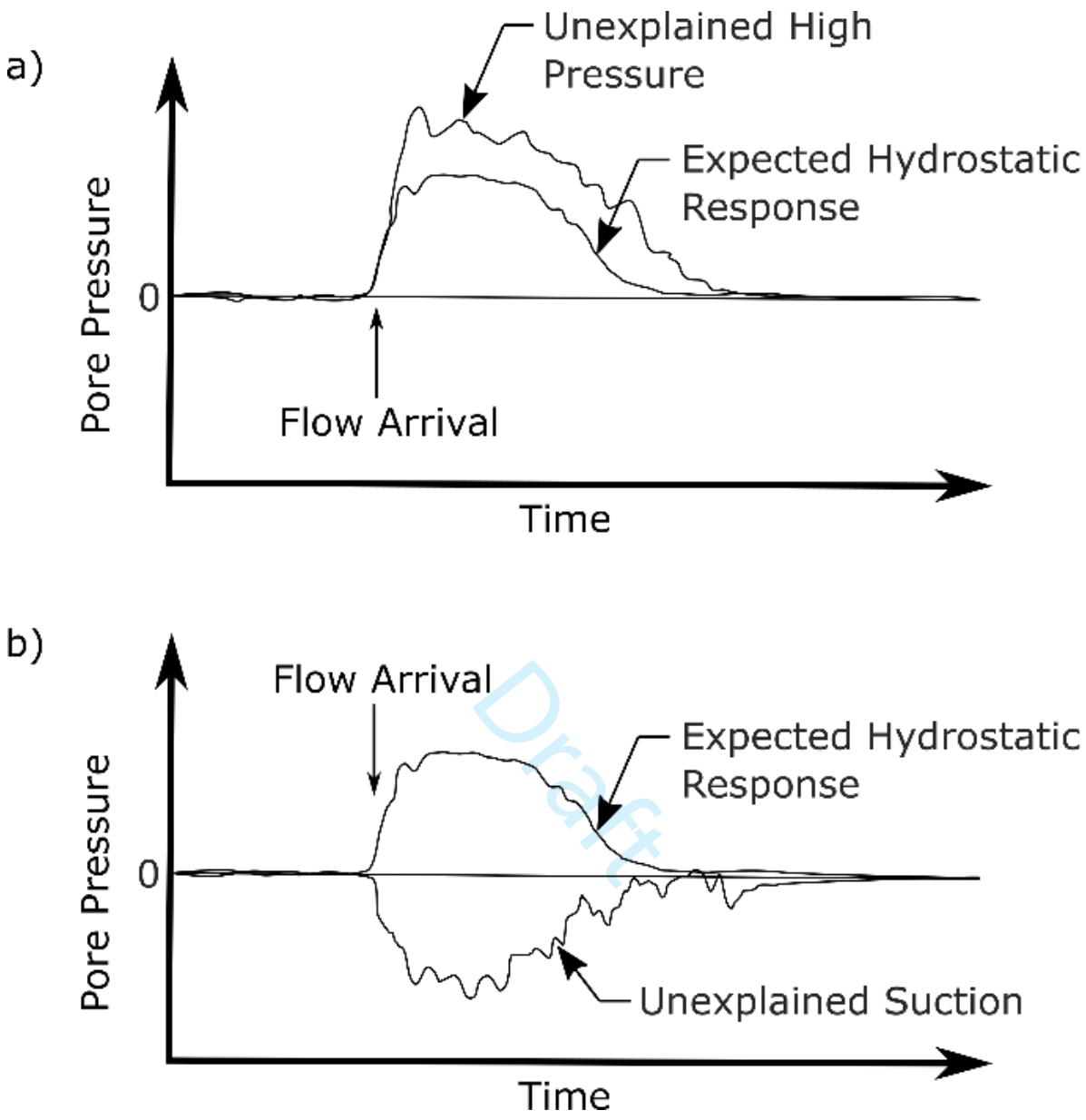

Figure 1 - Illustration of (a) high and (b) suction basal pore water pressure responses for a constant volume, fully saturated, hydrostatic material passing over in contrast to the expected hydrostatic response.

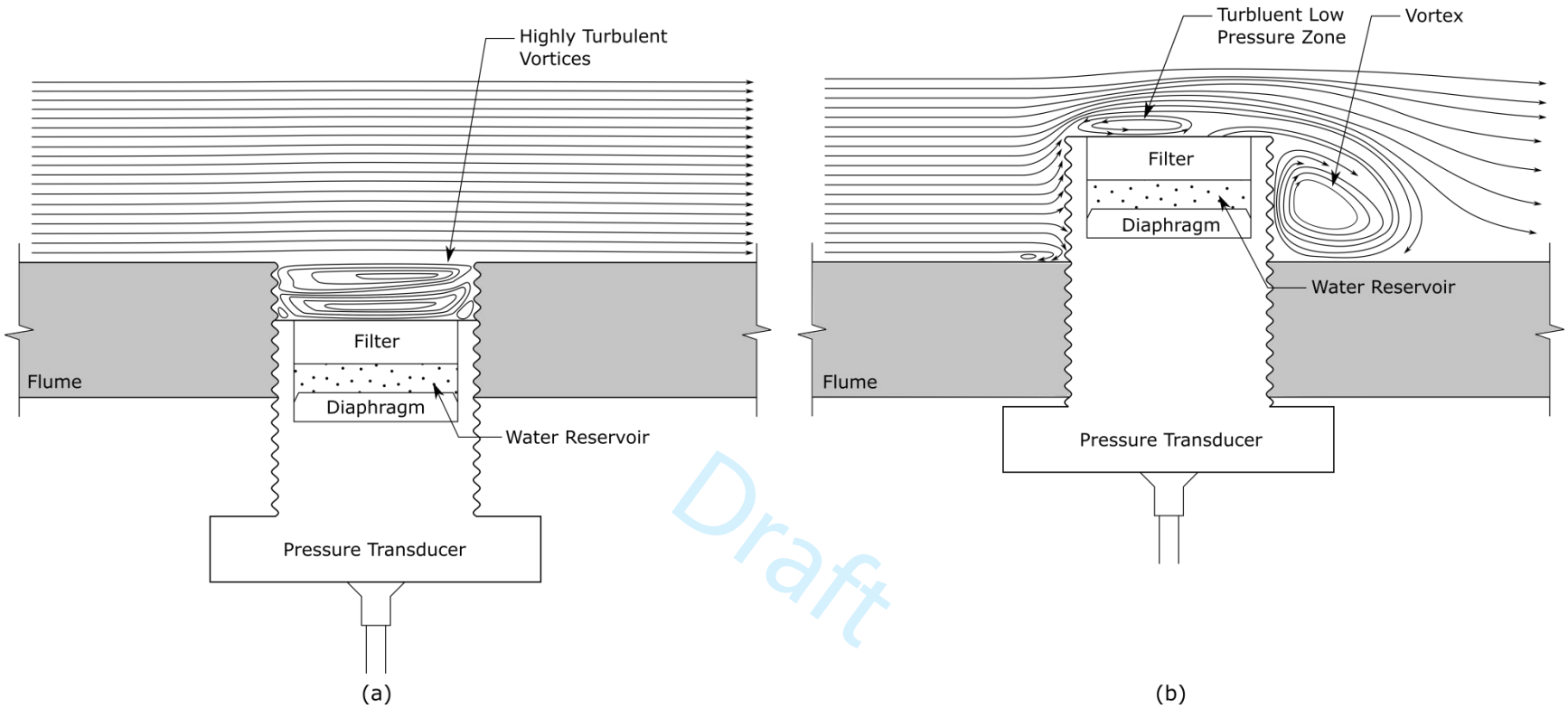

Figure 2 - Possible flow lines of material traveling (a) over a recessed cap (b) over a raised cap, both located above a PPT.

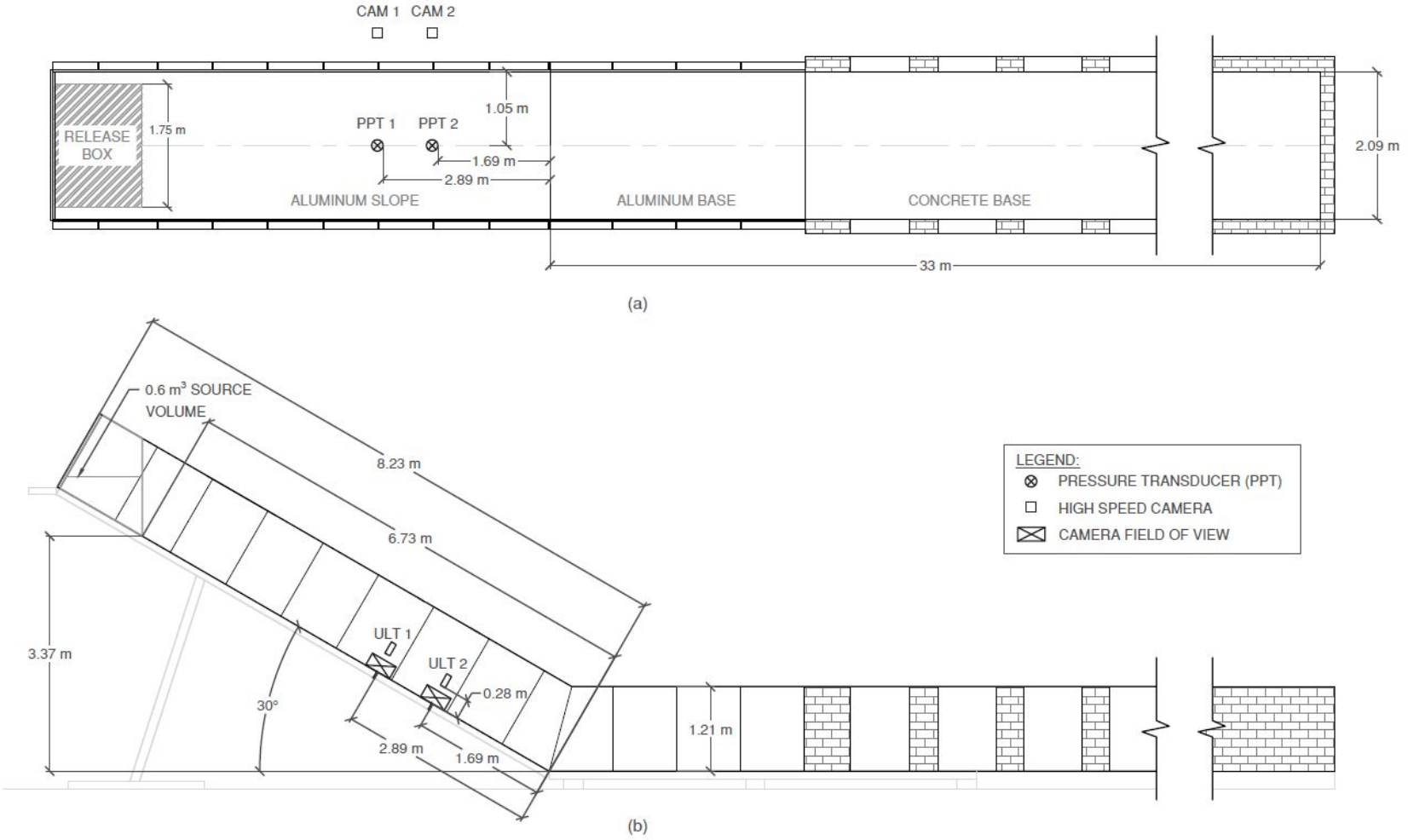

Figure 3 - Diagram of the (a) top and (b) side profile of the experimental flume setup with locations of instrumentation, including pore pressure transducers, ultrasonic sensors, and high speed cameras (with their side field of view displayed).

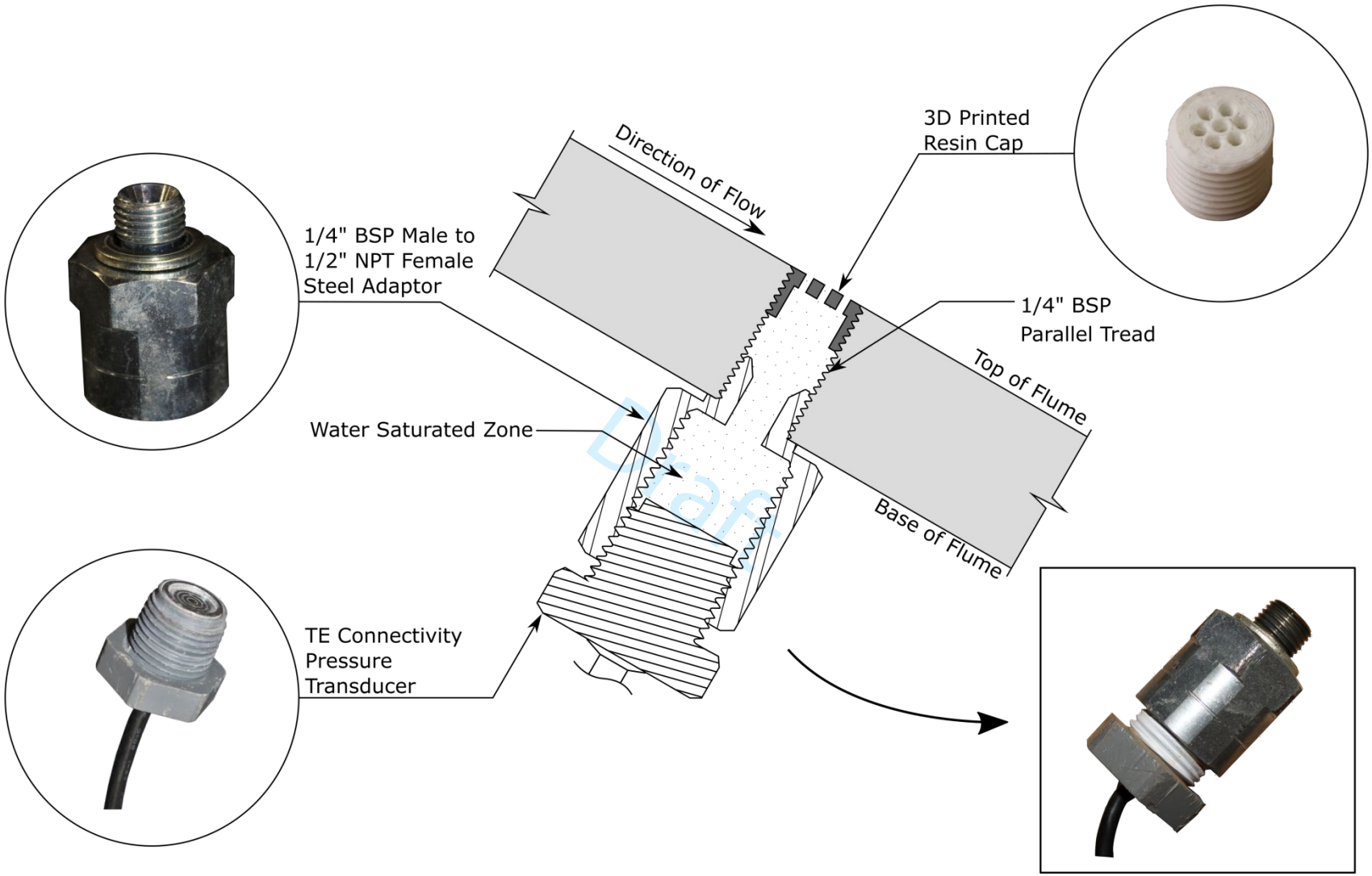

Figure 4 - Diagram of pore pressure transducer installation in the flume base with assembled configuration displayed.

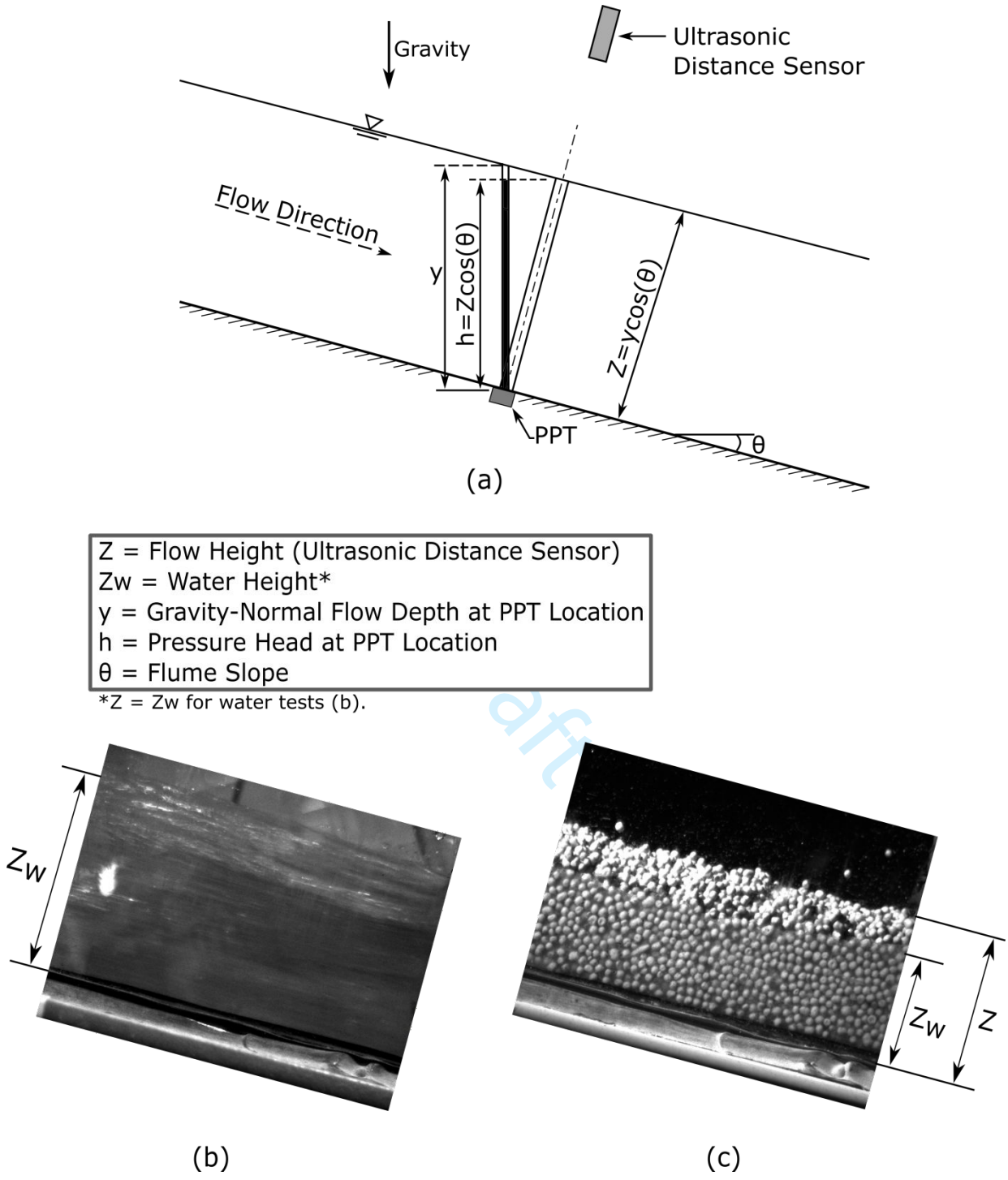

Figure 5 - (a) Definition of flow height measurement conventions, and theoretical pressure measurement h at PPT for a steady water flow, after Chow (1959). High speed image with flow (Z) and water (Zw) heights indicated for a (a) water test and (b) saturated, granular test.

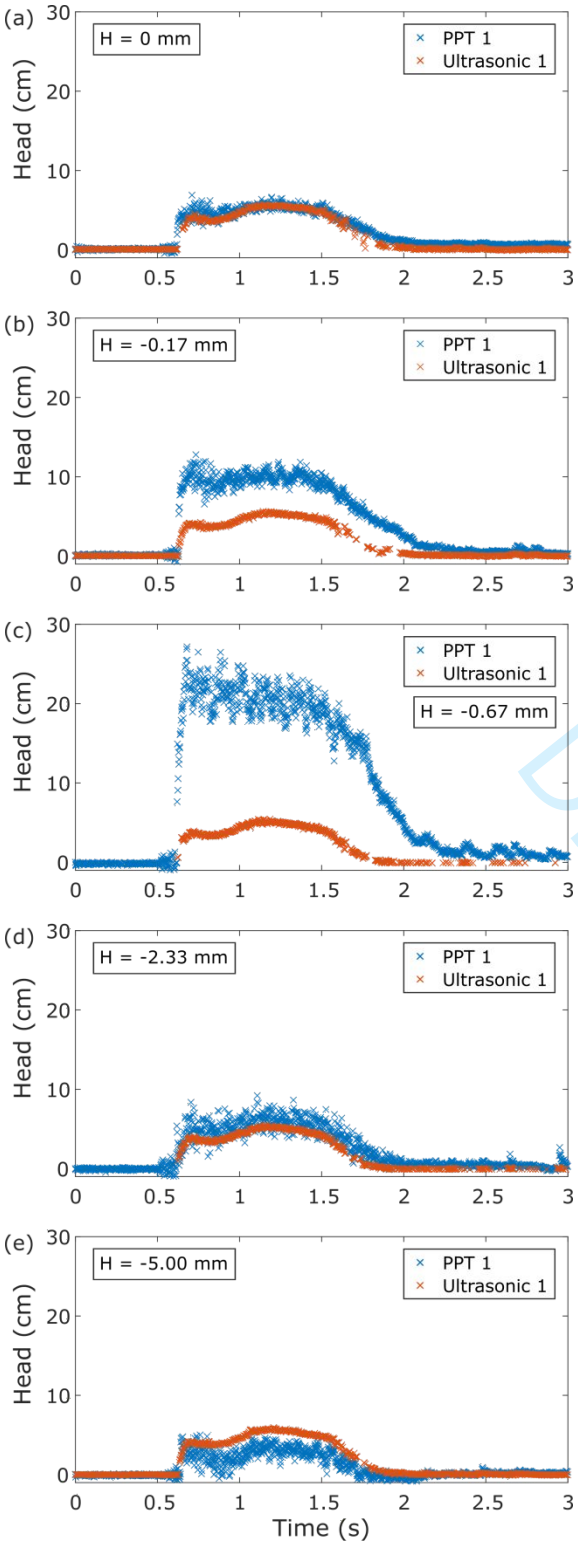

Figure 6 - PPT 1 and Ultrasonic 1 head versus time results for (a) a H = 0 mm Base reference test, and lowered cap tests with H of (b) -0.17 mm, (c) -0.67 mm, (d) -2.33 mm, and (e) -5.0 mm. Tests display the largest changes at small H's and then a decreasing difference until it passes through a false positive and becomes negative.

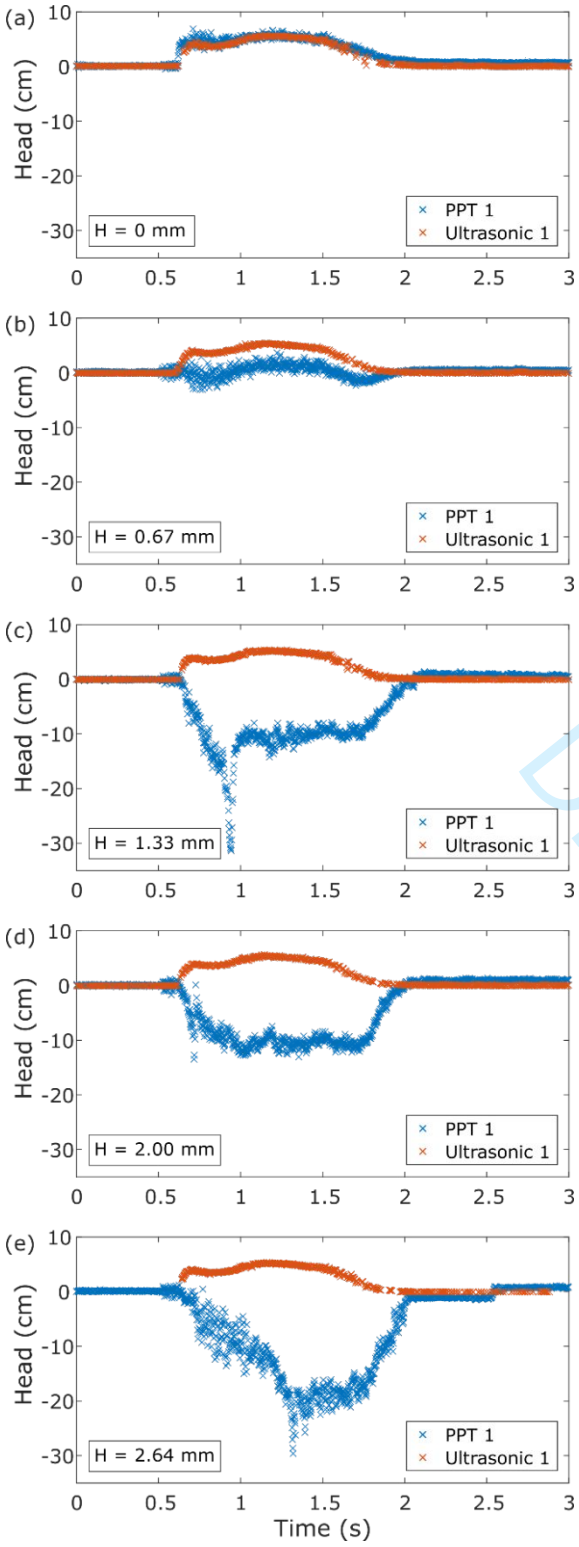

Figure 7 - PPT 1 and Ultrasonic 1 head versus time results for (a) a H = 0 mm Base reference test, and raised cap tests with H of (b) 0.67 mm, (c) 1.33 mm, (d) 2.0 mm, and (e) 2.64 mm. Tests display increasingly negative results as the cap is raised.

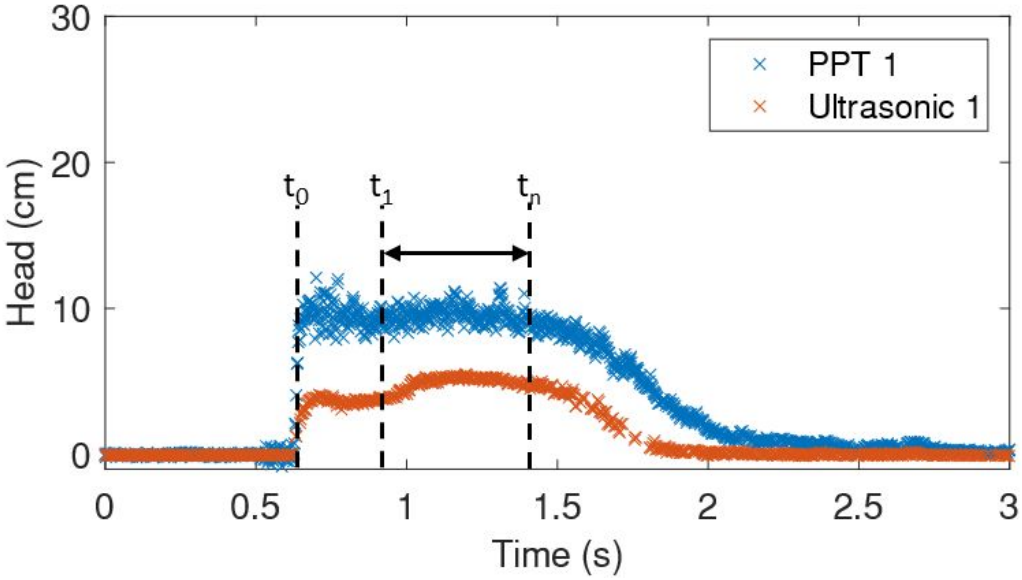

Figure 8 - Head versus time plot displaying the test time instances of wave arrival (t_0), start of sustained PPT maximum head (t_1), and end of sustained maximum head (t_n).

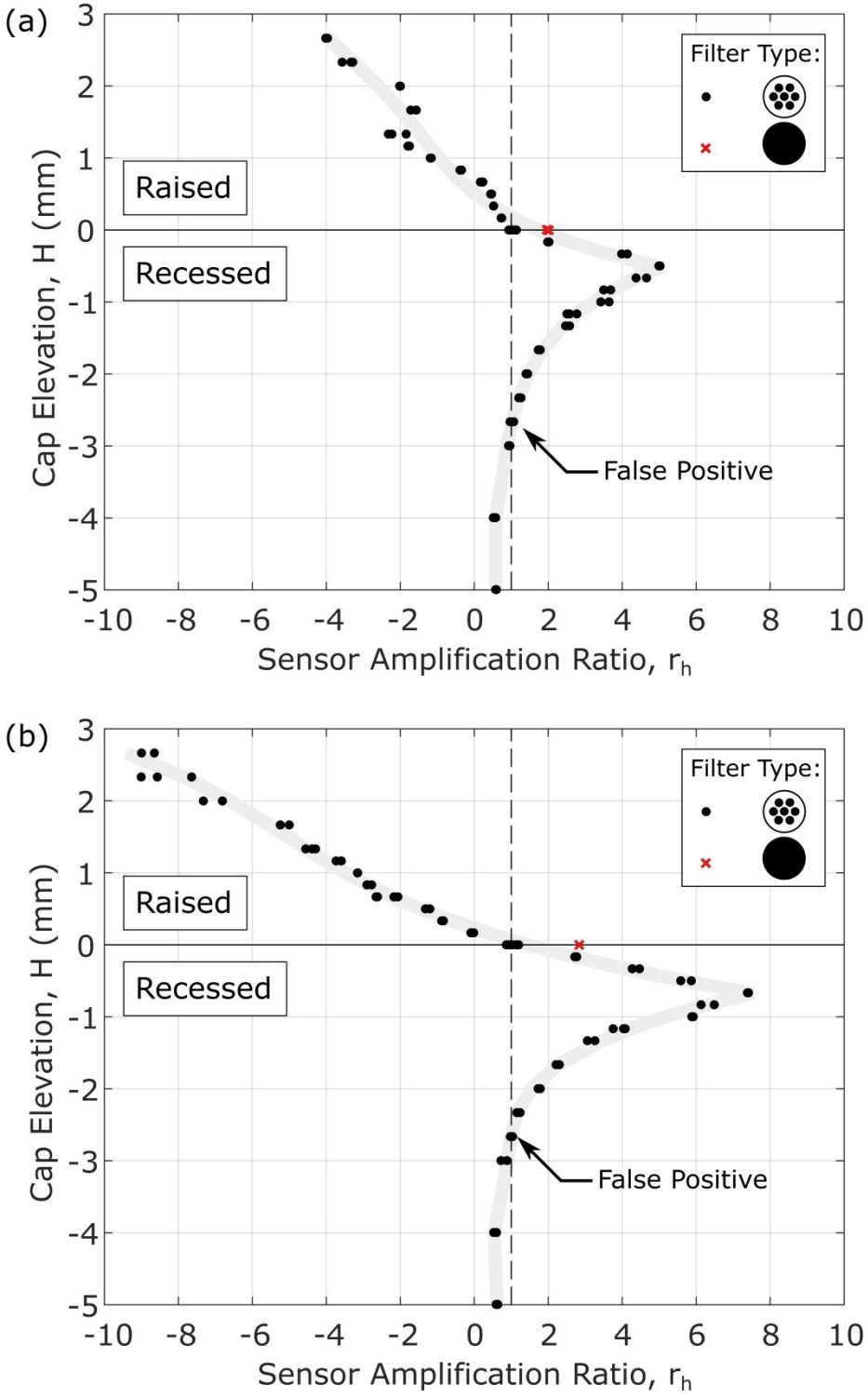

Figure 9 - Sensor amplification ratio, r_h versus cap elevation, H for (a) PPT 1 and (b) PPT 2 water tests. The dashed line indicates where the measured pressure results match the recorded ultrasonic flow height. The solid line indicates a perfectly flush cap height.

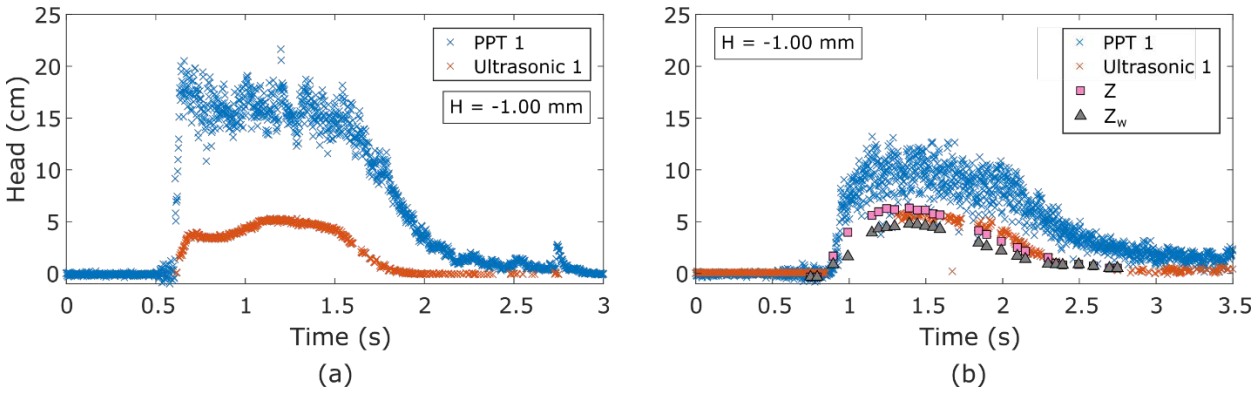

Figure 10 - Comparison between PPT 1 and Ultrasonic 1 head versus time results for (a) H = -1 mm water test and (b) H = -1 mm particle test, which also shows flow height (Z) and water height (Z_w) results.

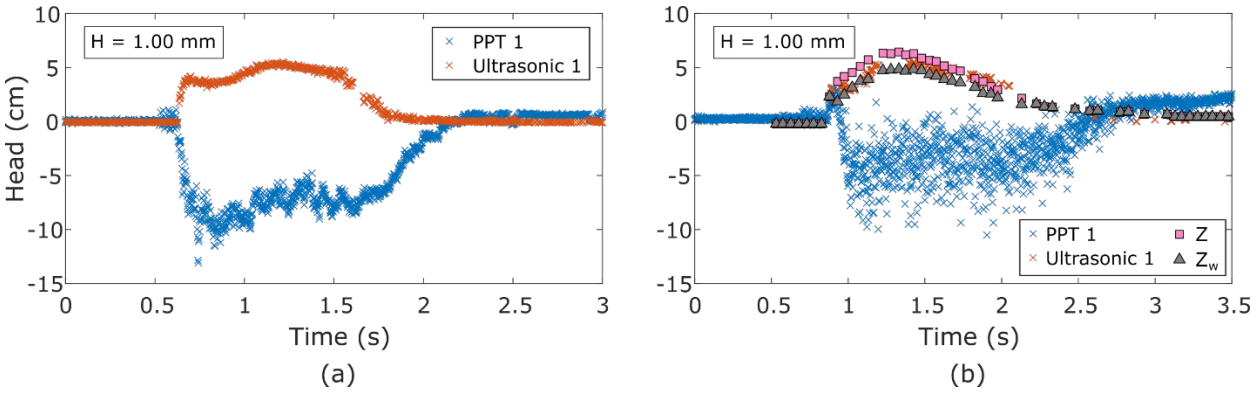

Figure 11 - Comparison between PPT 1 and Ultrasonic 1 head versus time results for (a) H = 1 mm water test and (b) H = 1 mm particle test, which also shows flow height (Z) and water height (Z_w) results.

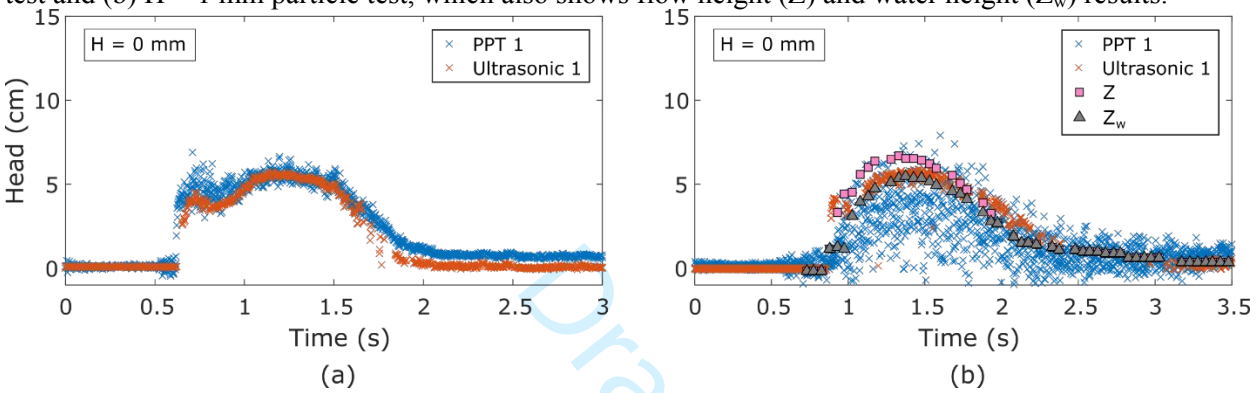

Figure 12 - Comparison between PPT 1 and Ultrasonic 1 head versus time results for (a) 0 mm water test and (b) 0 mm particle test, which additionally shows flow and water height results. Both display an agreement between the PPT and ultrasonic sensor results that suggest proper sensor setup.

Table 1 - Summary of tests.

Number of Tests	***Flow Material***	***Raised, Lowered, Flush, or No Cap Test***	***Cap Elevation, H (mm)***
8	Water	Flush	0.00
2	Water	Raised	0.17
2	Water	Raised	0.33
2	Water	Raised	0.50
4	Water	Raised	0.67
2	Water	Raised	0.83
2	Water	Raised	1.00
2	Water	Raised	1.17
3	Water	Raised	1.33
2	Water	Raised	1.67
2	Water	Raised	2.00
3	Water	Raised	2.33
2	Water	Raised	2.66
2	Water	Lowered	-0.17
2	Water	Lowered	-0.33
2	Water	Lowered	-0.50
2	Water	Lowered	-0.67
2	Water	Lowered	-0.83
2	Water	Lowered	-1.00
3	Water	Lowered	-1.17
2	Water	Lowered	-1.33
2	Water	Lowered	-1.67
2	Water	Lowered	-2.00
2	Water	Lowered	-2.33
2	Water	Lowered	-2.66
2	Water	Lowered	-3.00
24	Water	Lowered	-4.00

Number of Tests	*Flow Material*	*Raised, Lowered, Flush, or No Cap Test*	*Cap Elevation,* **H** *(mm)*
2	Water	Lowered	-5.00
2	Water	No Cap	0.00
1	3mm Particles & Water	Lowered	-1.00
1	3mm Particles & Water	Raised	1.00
2	3mm Particles & Water	Flush	0.00

Table 2 - Summary of Reynold's and Froude number calculations at PPT 1 and 2 in both the water and saturated granular flows.

	PPT 1		***PPT 2***	
	Water Tests	***Saturated Granular Tests***	***Water Tests***	***Saturated Granular Tests***
Flow Height, Z (m)	0.0530	0.0566	0.0435	0.0460
Flow Velocity (m/s)	6.13	4.00	7.02	5.00
Hydraulic Radius, R	0.0504	0.0537	0.0418	0.0441
Reynold's Number, Re	2.7×10^5	3.37×10^5	2.6×10^5	3.46×10^5
Froude Number, Fr	8.51	5.37	10.75	7.44